forum acusticum 2026
8-12 September · Graz, Austria

EFFECTS OF SPEED AND ACCELERATION ON OBSI TYRE–ROAD NOISE FOR ELECTRIC VEHICLES

Jiawen Meng[1], Frank Gauterin[2], Alexey Vinel[1,3]

[1] *Institute of Applied Informatics and Formal Description Methods (AIFB), Karlsruhe Institute of Technology (KIT), Germany*
[2] *Institute of Vehicle System Technology (FAST), Karlsruhe Institute of Technology (KIT), Germany*
[3] *School of Information Technology, Halmstad University, Sweden*

This paper is a revised version of the authors' submitted manuscript that was peer-reviewed by at least two anonymous reviewers.

Preliminary document

Abstract

With the increasing adoption of electric vehicles, tyre–road noise is becoming the dominant source of vehicle exterior noise at low and medium speeds. This study analyses on-board sound intensity (OBSI) data collected under constant-speed and acceleration conditions for five production tyres on three electric vehicles, measured on an ISO 10844:1994 reference surface.
The baseline speed dependence of OBSI levels is described using a log-linear mixed-effects model, confirming speed as the dominant factor governing tyre–road noise (9.9 dB per speed doubling, RMSE = 0.24 dB). Acceleration-related contributions, evaluated using a two-stage residual approach, show substantial variability across tyre–vehicle combinations, with no consistent overall effect and indications of confounding with vehicle characteristics.
The trailing–leading level difference exhibits a tyre-dependent speed sensitivity that shows a strong association with rolling resistance ($r = 0.95$, $p = 0.014$), supported by within-vehicle comparisons. These findings suggest a potential link between rolling resistance and the balance of leading- and trailing-edge noise generation mechanisms.

Keywords: *tyre–road noise, OBSI, electric vehicles, acceleration noise, trailing–leading balance*

1. Introduction

Road traffic is a major source of environmental noise exposure in Europe. Its health effects, particularly sleep disturbance and cardiovascular disease, are well documented [1], [2]. The increasing adoption of electric vehicles (EVs) has reduced propulsion noise, making tyre–road interaction the dominant source of vehicle noise, particularly at urban and medium speeds [3]. This makes it essential to understand how tyre–road noise (TRN) depends on operating conditions and tyre properties, both for physical interpretation and for noise reduction.

On-board sound intensity (OBSI) measurements capture acoustic radiation directly at the tyre–road interface and provide near-field information on TRN. By placing probes at the leading and trailing edges of the contact patch, they enable the separation of contributions from distinct source regions [4].

Previous studies have shown that acceleration can increase near-field tyre noise levels by several decibels depending on tyre design [5], and pass-by measurements have confirmed that this effect varies across tyre–vehicle combinations [6]. However, the continuous separation of speed and acceleration contributions to near-field tyre noise has not yet been systematically addressed. Similarly, while source localisation studies have shown that the leading and trailing edges of the contact patch contribute differently to TRN [7], the relationship between tyre properties and these directional characteristics remains largely unexplored, particularly in the context of OBSI measurements.

This study addresses these gaps by introducing a two-stage modelling framework to separate speed and acceleration effects in OBSI data, and by analysing directional noise characteristics in relation to static tyre properties.

The analysis is based on OBSI measurements from five production tyres on three EVs, collected within the TyRoN (Tyre Road Noise) project. The measurement framework and a physics-based OBSI-to-pass-by model are described in [8], while a complementary data-driven analysis of the pass-by measurements is presented in [9].

Corresponding author: *jiawen.meng@kit.edu.*
Copyright: *©2026 Jiawen Meng et al. This is an open-access article distributed under the terms of the Creative Commons Attribution 3.0 Unported License, which permits unrestricted use, distribution, and reproduction in any medium, provided the original author and source are credited.*

2. Measurement Data and Processing

The measurements were carried out on an ISO 10844:1994 compliant surface at the IKA test track in Aachen [10]. Five production tyres mounted on three EVs were investigated (Table 1). Since only one or two tyres were tested per vehicle, the experimental design is partially nested, which may introduce confounding between tyre and vehicle effects. For each test, TRN was measured at the right-rear wheel position using the OBSI method, with probes positioned at the leading and trailing edges of the contact patch. The probe setup follows the OBSI methodology, with adaptations to the lateral probe positioning as detailed in [8]. Vehicle speed, longitudinal acceleration, air temperature, and road surface temperature were recorded simultaneously.

Table 1: Tested tyres and vehicles.

ID	Tyre model	Size	Vehicle
T1	EcoContact 6 Q	235/55 R19	ID.4
T2	RainSport 5	235/55 R19	ID.4
T3	PremiumContact 6 AO	255/50 R20	Q8 e-tron
T4	Ventus S1 evo3 ev	255/50 R20	Q8 e-tron
T5	P-Zero	275/35 R21	Taycan

Two types of driving manoeuvres were performed (Table 2). Constant-speed passes at 45, 80, and 100 km/h were used as the baseline dataset. For the acceleration runs, the vehicle entered the measurement section at 50 km/h and was accelerated at target levels of 1, 2, and 3 m/s^2. Each combination of tyre and manoeuvre was repeated multiple times.

Table 2: Driving manoeuvres and test conditions.

Manoeuvre	Conditions
Constant speed	45, 80, 100 km/h
Acceleration	1, 2, 3 m/s^2, starting from 50 km/h

In addition, static tyre properties were determined for each tyre, including Shore A hardness, radial stiffness, footprint dimensions, circumference, rolling resistance, and tyre mass. These parameters were used in the exploratory analyses presented in Section 3.

All time-series signals were segmented into non-overlapping 0.25 s windows. For each window, speed and acceleration were obtained as arithmetic means, while the sound intensity signals were averaged in the linear domain (i.e. in W/m^2). The leading- and trailing-edge intensities were then combined to obtain the overall OBSI level:

$$L = 10 \log_{10}\left(\frac{I_{\text{lead}} + I_{\text{trail}}}{2\, I_0}\right), \tag{1}$$

where $I_0 = 10^{-12}\ \mathrm{W/m^2}$. After processing, the dataset comprised 481 observation windows for constant-speed conditions and 410 for acceleration runs.

3. Analysis and Results

3.1. Speed and Acceleration Effects on OBSI Level

To separate the speed dependence of rolling noise from any additional acceleration effect, a two-stage modelling approach was adopted. In the first stage, a linear mixed-effects model was fitted to the constant-speed data:

$$L_{ij} \;=\; \beta_0 + \beta_1 \log_{10} v_{ij} + u_{0j} + u_{1j} \log_{10} v_{ij} + \varepsilon_{ij}, \tag{2}$$

where L_{ij} is the windowed OBSI level of observation i on tyre j, v_{ij} is the vehicle speed, u_{0j} and u_{1j} are tyre-specific random intercept and slope allowing for differences in both overall noise level and speed sensitivity across tyres, and $\varepsilon_{ij} \sim \mathcal{N}(0, \sigma^2)$ is the residual error. Parameters were estimated by restricted maximum likelihood (REML).

Air and road surface temperatures were initially considered as additional predictors but were excluded from the final model. Measurements for each tyre were conducted on different days, with air temperatures ranging from approximately 15 to 25 °C across test days and little overlap between tyres, resulting in strong confounding between temperature effects and the tyre-specific intercepts. This exclusion is unlikely to affect the subsequent comparison, since constant-speed and acceleration runs for each tyre were conducted on the same day under nearly identical conditions (with a mean air temperature difference between constant-speed and acceleration runs of less than 1 °C for each tyre).

The baseline model yields a speed coefficient of $\hat{\beta}_1 = 33.0$ dB/decade, corresponding to approximately 9.9 dB per doubling of speed. The model provided a good fit to the constant-speed dataset within the tested range, with root mean square error (RMSE) of 0.24 dB. Differences among the tested tyre–vehicle combinations are captured by the random effects, as shown in Figure 1.

In the second stage, the baseline model was used to predict the expected level $\hat{L}_{ij}$ for the acceleration data. The residual

$$\Delta L_{ij} \;=\; L_{ij} - \hat{L}_{ij} \tag{3}$$

was interpreted as the acceleration-induced noise contribution beyond the baseline speed effect. The speed range of the acceleration data (approximately 47 – 70 km/h for all tyres) fell entirely within the range of the constant-speed data (42 – 100 km/h), ensuring that the Stage 1 predictions represent interpolation rather than extrapolation.

A second mixed-effects model with random intercept and slope per tyre was fitted to ΔL:

$$\Delta L_{ij} = \gamma_0 + \gamma_1\, a_{ij}^2 + b_{0j} + b_{1j}\, a_{ij}^2 + \epsilon_{ij}, \tag{4}$$

where a_{ij} is the longitudinal acceleration, b_{0j} and b_{1j} are tyre-specific random effects representing differences between tyres in overall level and sensitivity to acceleration, and ϵ_{ij} is the residual. The acceler-

Preliminary document

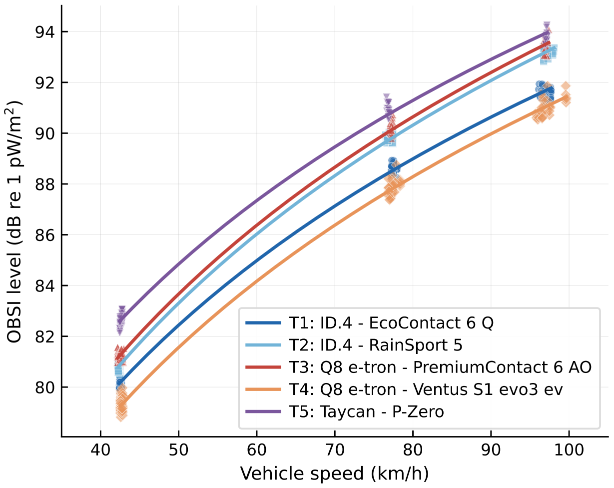

Figure 1: OBSI level vs. speed for each tyre (constant-speed data). Lines represent the fitted mixed-effects model (Eq. 2).

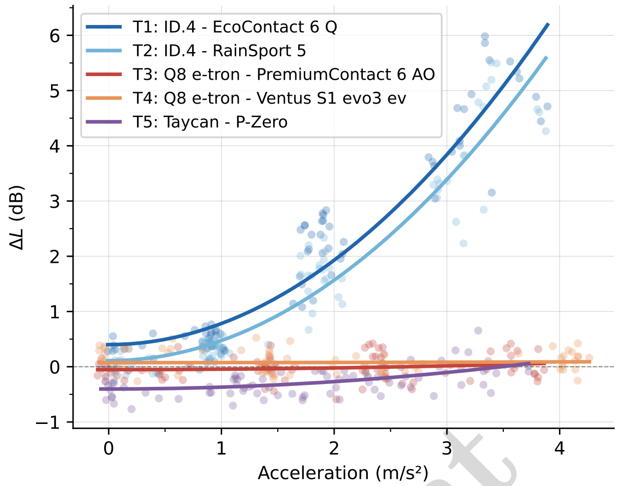

Figure 2: Acceleration-induced noise residual ΔL vs. longitudinal acceleration. Lines show the fitted model (Eq. 4) for each tyre.

ation term was modelled as a^2 rather than a, as the quadratic form provided a better fit.

The overall (average) effect of acceleration was not statistically significant ($\hat{\gamma}_1 = 0.158$, SE $= 0.088$, $p = 0.075$), suggesting that a single common effect does not adequately describe the data. Instead, tyre-specific slopes reveal substantial heterogeneity (Table 3, Figure 2): the two tyres measured on the ID.4 (T1 and T2) exhibited slopes of approximately 0.37–0.38 dB/(m/s^2)^2, whereas the three remaining tyres showed slopes below 0.04 dB/(m/s^2)^2. This suggests that the effect of acceleration varies across tyre–vehicle combinations.

Table 3: Tyre-specific acceleration slopes $\hat{\gamma}_1 + \hat{b}_{1j}$ [dB/(m/s^2)^2], sorted by descending magnitude.

Tyre	Model	Vehicle	Slope
T1	EcoContact	ID.4	0.382
T2	RainSport	ID.4	0.365
T5	P-Zero	Taycan	0.033
T3	PremiumContact	Q8 e-tron	0.008
T4	Ventus S1 evo3	Q8 e-tron	0.001

To explore whether this heterogeneity could be linked to tyre properties, the tyre-specific slopes were compared against the static tyre characteristics described in Section 2. Several parameters showed strong correlations with the acceleration slope, notably radial stiffness ($r = -0.98$, $p = 0.002$), footprint width ($r = -0.98$, $p = 0.004$), and tyre mass ($r = -0.94$, $p = 0.017$).

However, these correlations are likely spurious, as the parameters are themselves highly intercorrelated and only one or two tyres were tested per vehicle, confounding tyre and vehicle effects. This interpretation is supported by within-vehicle comparisons: for both the ID.4 (T1 vs. T2) and the Q8 e-tron (T3 vs. T4), the ranking of tyre properties did not match the ranking of acceleration slopes.

Separating these contributions would require a crossed experimental design with more tyres tested per vehicle.

3.2. Trailing–Leading Level Difference

The results in Section 3.1 indicate substantial variation in acceleration effects across tyre–vehicle combinations, but the underlying causes remain unclear. To gain additional insight into the directional characteristics of the noise generation, the trailing–leading level difference is examined in the following.

TRN is known to exhibit directional asymmetry, with different contributions from the leading and trailing edges of the contact patch. The OBSI method enables a comparison of sound levels at these two locations in the near field, providing an indication of this asymmetry. The quantity

$$\Delta L_i^{\mathrm{TL}} = L_i^{\mathrm{trail}} - L_i^{\mathrm{lead}}, \tag{5}$$

quantifies the balance between trailing- and leading-edge sound levels. Trailing-edge radiation is commonly associated with air pumping and tread snap-out, whereas leading-edge radiation is linked to tread impact and texture excitation. Positive values indicate that trailing-edge noise dominates.

Figure 3 shows that the absolute level of ΔL_{TL} varies considerably across tyres, with T2 and T4 showing trailing-edge dominance (positive values), T3 and T5 showing leading-edge dominance (negative values), and T1 remaining close to zero. The fitted lines also suggest that the speed dependence differs across tyres. To quantify this, per-tyre linear regressions were fitted:

$$\Delta L_i^{\mathrm{TL}} = \alpha_j + \beta_j \log_{10} v_i + \varepsilon_i, \tag{6}$$

where α_j and β_j are the intercept and slope for tyre j, and ε_i is the residual error. Separate regressions were used since the aim was to characterise individual tyre behaviour rather than estimate a population-level effect. The estimated slopes ranged from -0.22 dB per

Preliminary document

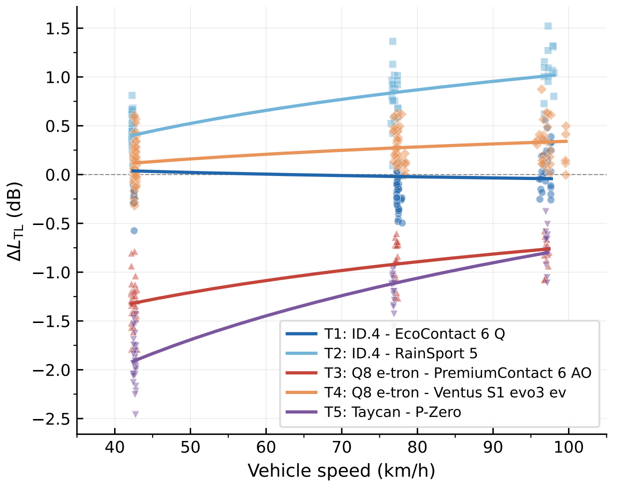

Figure 3: Trailing–leading level difference ΔL_{TL} vs. speed for each tyre (constant-speed data), with per-tyre linear regressions (Eq. 6).

decade for T1 to 3.09 dB per decade for T5 (Table 4).

Table 4: T–L speed slopes $\hat{\beta}_j$ and rolling resistance (RR).

Tyre	**Vehicle**	$\hat{\beta}_j$ [dB/decade]	**RR [kg/t]**
T5	Taycan	3.09	9.20
T2	ID.4	1.69	7.28
T3	Q8 e-tron	1.54	7.16
T4	Q8 e-tron	0.60	6.98
T1	ID.4	−0.22	4.51

Among the tyre properties examined, rolling resistance showed the strongest association with the T–L slope ($r = 0.95$, $p = 0.014$, $n = 5$; Figure 4). This trend was also consistent within vehicle groups: for both the ID.4 (T1 vs. T2: $\Delta\hat{\beta} = +1.91$, $\Delta\mathrm{RR} = +2.77\,\mathrm{kg/t}$) and the Q8 e-tron (T3 vs. T4: $\Delta\hat{\beta} = +0.94$, $\Delta\mathrm{RR} = +0.18\,\mathrm{kg/t}$), the tyre with higher rolling resistance exhibited a larger T–L speed slope. This within-vehicle consistency is in line with the observed trend, although the limited sample size precludes robust statistical inference.

A possible interpretation is that higher rolling resistance is associated with greater viscoelastic energy dissipation in the contact patch, which may enhance vibration or slip processes at the trailing edge. At higher speeds, these mechanisms are amplified, resulting in a steeper growth of the T–L difference. This should be regarded as a hypothesis to be tested in future campaigns with a larger and more balanced dataset.

Together with the results of Section 3.1, these observations highlight the substantial variability in TRN characteristics across the tyre–vehicle combinations tested in this study.

4. Conclusion

This study shows that the speed dependence of OBSI TRN can be well described by a log-linear mixed-

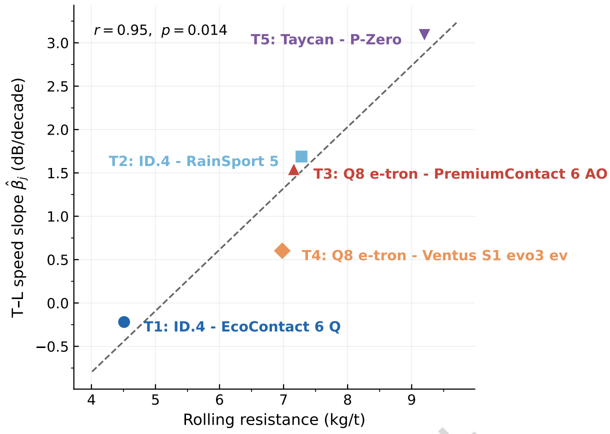

Figure 4: T–L speed slope $\hat{\beta}_j$ vs. rolling resistance ($r = 0.95$, $p = 0.014$, $n = 5$), with linear fit (dashed line).

effects model. The estimated population-level coefficient is 33.0 dB/decade, with an RMSE of 0.24 dB, confirming speed as the dominant factor governing OBSI levels.

Acceleration-induced contributions, evaluated using a two-stage residual approach, were not significant at the population level but exhibited substantial heterogeneity across tyre–vehicle combinations. Since only one or two tyres were tested per vehicle, the present data do not allow a robust separation of tyre and vehicle effects.

The trailing–leading level difference revealed distinct directional emission patterns across tyres. Its speed dependence showed a strong association with rolling resistance ($r = 0.95$, $p = 0.014$), a trend consistent across vehicle groups. A possible link to viscoelastic energy dissipation at the trailing edge is proposed as a hypothesis for further investigation.

Ongoing work within the TyRoN project aims to extend the dataset using a crossed tyre–vehicle design, enabling a robust separation of tyre and vehicle effects. In addition, detailed tyre structural and tread-related features will be incorporated as predictors to investigate the mechanisms governing noise generation under different operating conditions.

5. Acknowledgments

This publication is part of the "Tyre Road Noise" research project, which is funded by the German Federal Ministry for Digital and Modernization based on a decision of the German Bundestag (funding reference: 01F2269A). The authors thank the TyRoN project partners for providing the test vehicles, tyres, and measurement data.

References

[1] European Environment Agency, "Environmental noise in europe 2025," European Environment Agency, Tech. Rep., 2025. [Online]. Available: `https://www.eea.europa.eu/`

Preliminary document

en/analysis/publications/environmental-noise-in-europe-2025.

[2] S. Khomenko et al., "Impact of road traffic noise on annoyance and preventable mortality in european cities: A health impact assessment," *Environment International*, vol. 162, p. 107 160, 2022, ISSN: 0160-4120. DOI: 10.1016/j.envint.2022.107160.

[3] J. P. Arenas, "On the impact of electric vehicle transition on urban noise pollution," *Current Opinion in Environmental Science & Health*, vol. 45, p. 100 623, 2025, ISSN: 2468-5844. DOI: 10.1016/j.coesh.2025.100623.

[4] P. R. Donavan, *Measuring Tire-Pavement Noise at the Source* (NCHRP Report). Washington, DC, USA: Transportation Research Board, 2009, vol. 630.

[5] P. R. Donavan, "Tire-pavement interaction noise measurement under vehicle operating conditions of cruise and acceleration," in *SAE Noise & Vibration Conference & Exposition*, SAE Technical Paper 931276, SAE International, May 1993. DOI: 10.4271/931276.

[6] C. Hoever, A. Tsotras, M.-A. Pallas, and J. Cesbron, "Factors influencing tyre/road noise under torque," in *Proceedings of the INTER-NOISE and NOISE-CON Congress and Conference*, vol. 265, Institute of Noise Control Engineering, 2023, pp. 3683–3690.

[7] R. J. Ruhala and C. B. Burroughs, "Localization of tire/pavement noise source regions," *Noise Control Eng. J.*, vol. 56, no. 5, pp. 318–331, 2008.

[8] M. G. Winter, C. Schliephake, G. Böttcher, V. Yordanov, and D. Werner, "Integrated acoustic measurement framework for tyre-road noise analysis," in *Proceedings of the Aachen Acoustics Colloquium*, 23–25 November 2025, Aachen, Germany, Nov. 2025.

[9] J. Meng, F. Gauterin, and A. Vinel, "Interpretable tyre-road noise prediction using structured multimodal machine learning," in *Proceedings of the Aachen Acoustics Colloquium*, 23–25 November 2025, Aachen, Germany, Nov. 2025.

[10] *ISO 10844:1994 Acoustics – Specification of test tracks for measuring noise emitted by road vehicles*, International Organization for Standardization (ISO), 1994.

Preliminary document